encit 2020

ABCM Associação Brasileira de Engenharia e Ciências Mecânicas

18th Brazilian Congress of Thermal Sciences and Engineering
November 16-20, 2020 (Online)

ENC-2020-0635
STATE ESTIMATION USING THE OPTIMAL SEQUENTIAL BAYESIAN FILTER IN BIOHEAT TRANSFER APPLICATIONS

Felipe Sant'Anna Nunes
Federal University of Rio de Janeiro – UFRJ/COPPE, Program of Mechanical Engineering, Rio de Janeiro, RJ, Brazil
fsantannan@mecanica.coppe.ufrj.br

Felipe Yamaguchi Magalhães
Federal University of Rio de Janeiro – UFRJ/COPPE, Program of Mechanical Engineering, Rio de Janeiro, RJ, Brazil
fyamaguchi@mecanica.coppe.ufrj.br

Nilton Pereira da Silva
Federal University of Rio de Janeiro – UFRJ/COPPE, Program of Mechanical Engineering, Rio de Janeiro, RJ, Brazil
Federal University of Amazonas – UFAM/DEMEC, Department of Mechanical Engineering, Manaus, AM, Brazil
niltonps@ufam.edu.br

Helcio Rangel Barreto Orlande
Federal University of Rio de Janeiro – UFRJ/COPPE, Department of Mechanical Engineering, Rio de Janeiro, RJ, Brazil
helcio@mecanica.coppe.ufrj.br

Abstract. *The Optimal sequential Bayesian filter is used to solve state estimation problems for low-dimensional, smooth systems. In this paper, two simulated bioheat transfer applications are presented. The first case involves the heating of one well in a 96-well plate, with a NIR laser during six minutes. The culture well contains 260 microliters of nanofluid with absorption coefficient 437.5 m^{-1}. The lateral and bottom surfaces of the well were considered thermally insulated and the top surface exchanged heat with the surroundings by convection and linearized radiation. The medium was assumed to be at a uniform temperature and natural convection effects were neglected. The second case presented concerns the system of body temperature regulation in living beings, especially in endothermic species. In order to evaluate the renal contribution in body thermoregulation, the Bayesian filter was used to estimate the energy source term resulting from renal metabolic activity, from simulated transient measurements of urine temperature. The energy generation (ATP) for a certain renal consumption of glucose and oxygen was quantified using a tool package for Matlab named COBRA. The results obtained with simulated measurements reveal that Optimal sequential Bayesian filter is an effective solver for state estimation for both analyzed cases.*

Keywords: *Inverse problems, state estimation, hyperthermia and renal metabolism*

1. INTRODUCTION

Unknown model parameters or functions can be estimated with the experimental responses of the system via inverse analysis (Ozisik and Orlande, 2000). Kaipio and Somersalo (2004) call the problems associated with state estimation as non-stationary inverse problems. Fox et al. (2019a) developed the Optimal sequential Bayesian filter and through numerical examples show that the method is effective and providing convergent estimates of the desired dynamic variables.

The Optimal sequential Bayesian filter presented in this work, developed by Fox et al. (2019a), is used for state estimation in two distinct bioheat transfer problems. The filter requires solving an advection equation for the state variables, which is done with the finite volume method. To perform this sequential Bayesian inference, let us consider a generic dynamical system that evolves according to the differential equation given by

$$\frac{d}{dt}\mathbf{x} = f(\mathbf{x}) \tag{1}$$

where $\mathbf{x}(t)$ is the state vector at time t and $f(\mathbf{x})$ is a known velocity field. Equation (1) can be solved deterministically to determine the future state $\mathbf{x}(t)$ when an initial state $\mathbf{x}(0) = \mathbf{x}_0$ is given. However, when the initial

state is uncertain, the future state is also uncertain. For the given system, measurements $\mathbf{z}_k$ are considered available at times t_k for $k = 1, 2, 3, \ldots$, providing noisy information about the state vector $\mathbf{x}_k = \mathbf{x}(t_k)$.

Let us now assume that the measurement process and the statistics of the measurement noise are known, i.e., the conditional distribution over the measurements $\mathbf{z}_k$ given the state vector $\mathbf{x}_k$ is

$$\rho(\mathbf{z}_k \mid \mathbf{x}_k) \tag{2}$$

The formal Bayesian solution corresponds to determining the time-varying sequence of filtering distributions

$$\rho(\mathbf{x}_k \mid \mathbf{Z}_t) \tag{3}$$

over the state at time t conditioned on all measurements to time t. Where $\mathbf{Z}_t$ denotes all the observation up to time t. In addition, uncertainty in the state is modelled as a probability distribution over the state.

The approach taken by Fox et al. (2018) is to treat the continuous-time problem in Eq. (1) and (2) directly and to define a family of numerical approximations that converge in distribution to the continuous-time probability density function in Eq. (3). The family of time-varying probability density functions or filtering distributions given in Eq. (3) may be generated with sequential Bayesian inference iterating two steps (Jawinski, 1970 cited in Fox et al., 2019b). Those steps are: prediction and update.

In the prediction step, between measurement times t_k and t_{k+1}, $\mathbf{Z}_t$ is constant and the continuous-time evolution of the filtering distribution may be derived from the forward Chapman-Kolmogorov equation (Fox et al., 2018).

$$\rho(\mathbf{x}_{t+\Delta t} \mid \mathbf{Z}_{t+\Delta t}) = \rho(\mathbf{x}_{t+\Delta t} \mid \mathbf{Z}_t) = \int \delta(\mathbf{x}_{t+\Delta t} - \mathbf{x}(\Delta t; \mathbf{x}))\rho(\mathbf{x}_t \mid \mathbf{Z}_t) d\mathbf{x}_t \tag{4}$$

where δ is the Dirac delta. The deterministic solution mentioned before was used for Eq. (1). From Eq. (4), a linear operator on the space of probability distributions is defined (Fox et al., 2018), written as

$$S_{\Delta t} : \rho(\mathbf{x}_t \mid \mathbf{Z}_t) \mapsto \rho(\mathbf{x}_{t+\Delta t} \mid \mathbf{Z}_t) \tag{5}$$

where $S_{\Delta t}$ is named the Frobenius-Perron operator associated with Eq. (1) for time increment Δt. More information regarding the Frobenius-Perron operator can be found in Jawinski (1970); Fox et al. (2018) and Fox et al. (2019b).

In the update step, at measurement times t_k, $\mathbf{Z}_t$ changes from $\mathbf{Z}_{k-1}$ to $\mathbf{Z}_k$. The filtering distribution changes according to Bayes' theorem, written at observation time t_k as (Arulampalam et al., 2002).

$$\rho(\mathbf{x}_k \mid \mathbf{Z}_k) = \frac{\rho(\mathbf{x}_k \mid \mathbf{Z}_{k-1})\rho(\mathbf{z}_k \mid \mathbf{x}_k)}{\rho(\mathbf{z}_k \mid \mathbf{Z}_{k-1})} \tag{6}$$

where $\rho(\mathbf{x}_k \mid \mathbf{Z}_k)$ is the posterior probability density; $\rho(\mathbf{x}_k \mid \mathbf{Z}_{k-1})$ represents the prior, which incorporates all the uncertainties of the unknown states without the information transmitted from the observations; $\rho(\mathbf{z}_k \mid \mathbf{x}_k)$ is the likelihood function, which incorporates the uncertainties of the measurements; and $\rho(\mathbf{z}_k \mid \mathbf{Z}_{k-1})$ is a normalizing constant. The likelihood function, $\rho(\mathbf{z}_k \mid \mathbf{x}_k)$, may be written as (Orlande, 2015).

$$\rho(\mathbf{z}_k \mid \mathbf{x}_k) = \exp\left[-\frac{1}{2}\left(\frac{(\mathbf{z}_k - \mathbf{x}_k)}{\sigma_{meas}} \right)^2 \right] \tag{7}$$

The Frobenius-Perron operator is responsible to evolve the filtering density forward in time. It can be written as the solution of an initial value problem in a partial differential equation for the probability density function. When equating the rate of change in the probability density function with the rate at which probability mass enters a delimited infinitesimal region, the given continuity equation is obtained (Fox et al., 2019b)

$$\frac{\partial}{\partial t}\rho = -\nabla.(\rho f) \tag{8}$$

The partial differential Eq. (8) is a linear advection equation and may be solved with initial condition $\rho(\mathbf{x};0)=\rho(\mathbf{x}_t \mid \mathbf{Z}_t)$ to evaluate $\rho(\mathbf{x};\Delta t)=\rho(\mathbf{x}_{t+\Delta t} \mid \mathbf{Z}_t)$ (Fox et al., 2019b).

The finite volume method in its explicit form is used to solve Eq. (8) (Patankar, 1980). In its integral form, the discretization of the continuity equation in the state space K may be represented as

$$\frac{\partial}{\partial t}\int_K (\rho)d\mathbf{x} = -\int_K (\rho f)d\mathbf{x} \tag{9}$$

The use of the upwind scheme for the discretization of Eq. (9) makes essential to evaluate the direction of flow in each problem. The method should also satisfy the Courant-Friedrichs-Lewy (CFL) stability criteria, presented in Fox et al. (2019b), which assures that positivity is preserved at each iteration in finite volume method.

2. LASER HEATING FOR HYPERTHERMIA

Previous works can be cited as a brief background for the given problem. In Tang and McGoron (2009) a laser was used to heat cancer cells in vitro in the presence of a photothermal agent (indocyanine green) to evaluate the cytotoxic effect of hyperthermia combined with chemotherapy. In Varon et al. (2020) the photothermal effect of iron oxide (Fe_2O_3) nanoparticles dissolved in distilled water and heated by a laser in the near infrared range was evaluated. It was observed that the temperature increase is directly proportional to the concentration of nanoparticles. More information regarding the application of the inverse analyses in cancer therapy problems by hyperthermia can be found in Varon et al. (2016) and Lamien et al. (2017).

2.1 Mathematical formulation

The given problem consists in the laser heating of one well in a 96-well plate as illustrated in Fig. 1. The medium was considered homogeneous and the initial temperature was assumed uniform. The lateral and bottom surfaces of the well were considered thermally insulated while the top surface was considered to exchange heat with the surroundings by convection. The temperature gradients and natural convection effects were neglected.

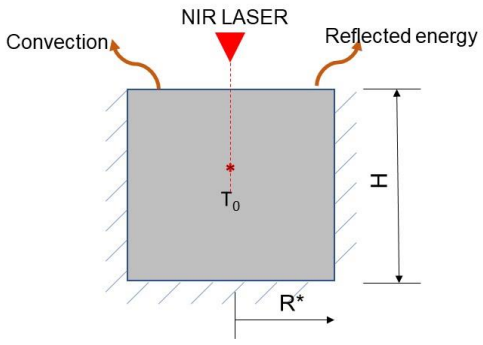

Figure 1. Sketch of the laser heating of one well in a 96-well plate

The mathematical formulation of the hyperthermia problem is thus given by

$$\frac{dT}{dt}+\left[\frac{h}{\rho C_p H}\right]T=\left[\frac{S_{laser}}{\pi R^{*2}\rho C_p H}\right]+\left[\frac{hT_\infty}{\rho C_p H}\right] \tag{10}$$

where

$$S_{laser}=[1-R]\left(\frac{2P_{laser}}{\pi r_{laser}^{\ 2}}\right)\mu_\alpha 2\pi\left\{\left[\frac{1}{\mu_\alpha}\right]-\left[\frac{e^{(-\mu_\alpha H)}}{\mu_\alpha}\right]\right\}\left\{\left[\frac{r_{laser}^{\ 2}}{4}\right]-\left[\left(\frac{r_{laser}^{\ 2}}{4}\right)e^{\left(-\frac{2R^{*2}}{r_{laser}^{\ 2}}\right)}\right]\right\} \tag{11}$$

Equation (10) can be rewritten as

$$\frac{dT}{dt}+\left[\frac{P_{hc}}{H}\right]T=\left[\frac{P_{sc}}{\pi R^{*2}H}\right]+\left[\frac{P_{hc}T_{\infty}}{H}\right] \tag{12}$$

where

$$P_{hc}=\frac{h}{\rho C_p}\;;\; P_{sc}=\frac{S_{laser}}{\rho C_p} \tag{13a-b}$$

The analytical solution of the model is given by

$$T(t)=e^{(-AT)}T_0+\frac{B}{A}\left[1-e(-At)\right] \tag{14}$$

where

$$A=\frac{P_{hc}}{H}\;;\; B=\left[\frac{P_{sc}}{\pi R^{*2}H}+\frac{P_{hc}T_{\infty}}{H}\right] \tag{15a-b}$$

and ρ is the density, C_p is the specific heat and r_{laser} is the laser beam.

The dynamics of the problem is described by Eq. (1) where the state vector and the velocity field are given by

$$\mathbf{x}=[T]\;;\; \frac{d}{dt}[T]=f[T]=[f_1(T)] \tag{16a-b}$$

The space state was discretized with n = 100. The range of T was restricted to (T_{inf} , T_{sup}).

3. KIDNEY PROBLEM

The uniform body temperature in endothermic species is maintained by thermogenesis, which is directly related to the cellular metabolism (Ricquier, 2016). Lutaif et al. (2008) presented experimental results that revealed the important role of kidneys in the body thermoregulation. These results suggested that the hypothermia observed in the nephrectomized rats (Sprague-Dawley) has been caused by the small metabolic heat generation due to the partial removal of the kidneys, which is compensated by the activation of the facultative thermogenesis that consumes the Brown Adipose Tissue (BAT). It has also been demonstrated that the main mechanism that activates the facultative thermogenesis is due to the kidney efferent nerval system, since the denervated animals had small masses of BAT even with the kidneys fully preserved. Therefore, there are strong experimental evidences that the kidneys and the renal neural pathways have an important role in the body thermoregulation, beyond the classically known kidney's functions. In this context, the model used in this section was proposed by Orlande et al. (2019).

3.1 Mathematical formulation

The proposed model considers a single kidney, as a body of homogeneous composition and uniform temperature. Mass and energy balances are written for a control volume surrounding the kidney. The model includes mass transfer processes to/from this control volume, which involve the flow of arterial blood (mass entry), venous blood, and urine (mass exit). Blood and urine are considered as homogeneous fluids. Figure 2 shows a schematic drawing of the renal model used in this work.

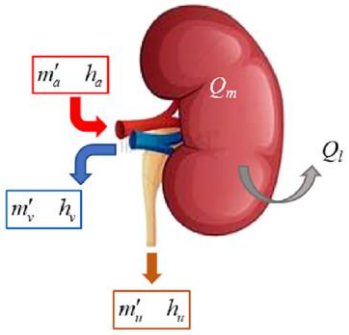

Figure 2. Sketch of the kidney model, adapted from Orlande et al. (2019)

Based on the problem represented in Fig. 2 and the considerations above, the energy balance and the mass balance can be written, respectively, as

$$\frac{d[m_k(t)e(t)]}{dt} = m'_a(t)h_a(t) - m'_v(t)h_v(t) - m'_u(t)h_u(t) + Q_m(t) - Q_l(t) \text{ in } V_k \text{ for } t > 0 \tag{17}$$

$$\frac{d[m_k(t)]}{dt} = m'_a(t) - m'_v(t) - m'_u(t) \tag{18}$$

where m is the mass, e represents the specific internal energy of the kidney, m' and h denote mass flow rate and specific enthalpy, respectively. The subscripts k, a, v and u represent the kidney, the arterial blood, the venous blood, and urine, respectively, while Q_m and Q_l are respectively the metabolic heat generation rate in the kidney, and the heat transfer rate lost from the kidney to the surroundings.

The kidney mass and the blood and urine mass flow rates are also considered constant in this work. Therefore, the mass balance can be written as follows

$$m'_v(t) = m'_a(t) - m'_u(t) \tag{19}$$

The heat transfer rate lost from the kidney to the surrounding organs and tissues is modeled in terms of a global heat transfer coefficient, U, that is,

$$Q_l = UA[T_k(t) - T_s], \tag{20}$$

where A is the surface area of the kidney and T_S is the temperature of the tissues / organs around the kidney, which is assumed as constant.

The renal artery is gradually divided into arterioles, which then converge to the venous system that progressively form the renal vein (Guyton and Hall, 2016). Such a small system, distributed throughout the kidney, leads to the hypothesis of a complete heat transfer, that is, the temperature of the venous blood is the same as the kidney temperature. The same hypothesis is used for urine, since it is formed by the process of filtration, reabsorption and secretion (Guyton and Hall, 2016). Therefore, we assume in our model that $T_k(t) = T_v(t) = T_u(t)$ so that we can rewrite Eq .17 as

$$\frac{d[T_k(t)]}{dt} = \frac{m'_a c_b}{m_k c_k} T_a(t) - \frac{(m'_a - m'_u) c_b}{m_k c_k} T_k(t) + \frac{Q_m(t)}{m_k c_k} + \frac{UA}{m_k c_k} T_s(t) - \frac{m'_u c_u + UA}{m_k c_k} T_k(t) \tag{21}$$

with initial condition given by a uniform temperature inside the kidney

$$T_k = T_{k,0} \text{ in } V_k \text{ for } t = 0, \tag{22}$$

where c is the specific heat and the subscript b refers to the blood.

The equation parameters can be defined as follows

$$\alpha = \frac{m'_u c_u}{m_k c_k} \; ; \; \beta = \frac{m'_a c_b}{m_k c_k} \; ; \; \gamma = \frac{(m'_a - m'_u) c_b}{m_k c_k} \; ; \; \varphi = \frac{1}{m_k c_k} \; ; \; \psi = \frac{UA}{m_k c_k} \tag{23a-e}$$

Therefore, the equation that governs the kidney problem can be rewritten according to the parameters in Eq.(23a-e) as

$$\frac{dT_k(t)}{dt} + (\alpha + \gamma + \psi) T_k(t) = \beta T_a(t) + \varphi Q_m(t) + \psi T_s(t) \tag{24}$$

The dynamics of the problem is described by Eq. (1) where the state vector and the velocity field are given by

$$\mathbf{x} = \begin{bmatrix} T \\ Q_m \end{bmatrix} \; ; \; \frac{d}{dt}\begin{bmatrix} T \\ Q_m \end{bmatrix} = f\begin{bmatrix} T \\ Q_m \end{bmatrix} = \begin{bmatrix} f_1(T, Q_m) \\ f_2(T, Q_m) \end{bmatrix} \tag{25a-b}$$

where $f_1(T, Q_m)$ is described by the Kidney Lumped model Eq. (25) while $f_2(T, Q_m)$ is described by the Random Walking model for the rate of metabolic heat generation in the kidney. This Random Walking model is described as follows

$$Q_m^{k+1} = Q_m^k + \varepsilon \; ; \; \frac{dQ_m}{dt} = \frac{\varepsilon}{\Delta t} \tag{26a-b}$$

where ε is a Gaussian distribution in (Q_m^k, σ^k), $\varepsilon \sim N(0, \sigma^k)$ with $\sigma^k = 2 \times 10\text{-}7$.

Therefore, one can write

$$\frac{dT_k}{dt} = f_1(T, Q_m) = -(\alpha + \gamma + \psi)T_k(t) + \beta T_a(t) + \varphi Q_m(t) + \psi T_s(t) \tag{28}$$

$$\frac{dQ_m}{dt} = f_2(T, Q_m) = \frac{\varepsilon}{\Delta t} \tag{29}$$

The space state was discretized with a uniform square mesh n x n with n = 50. The range of T was restricted to $(T_{\inf}, T_{\sup})$ while Q_m was restricted to $(Q_{m,\inf}, Q_{m,\sup})$.

4. RESULTS AND DISCUSSIONS

4.1 Laser heating for hyperthermia

The problem presented in section 2.1 was solved analytically, according to Eq. (14). Its numerical verification was performed using the routine ode15s, available in the commercial software Matlab. The height of the well is 0.007266 m with a radius of 0.003375 m. The density and specific heat of the medium are 997.07 kg/m^3 and 4180.9 J/kgK, respectively. Initially, the medium is at 37°C and exchanges heat with the environment at 25°C with a heat transfer coefficient of 8 W/m^{2}K. The heating of the well is produced by a laser beam with the given properties: r_{laser} = 0.00155 m, P_{laser} = 0.21928 W, μ_α = 437.5 m^{-1}, R = 0,02.

For the estimations obtained with the Optimal-Bayes filtering, the initial probability density function $\rho(\mathbf{x}_0)$ was considered Gaussian N (T_0, 0.5). The solution of the problem along the state space was discretized with n = 100 and its range was restricted to T_{inf} = 0°C and $T_{sup} = 1.1T_{max}$, where T_{max} is the maximum temperature of direct problem, as seen Fig. 4.

The evolution of the probability density function in time for the filtering states is shown in Fig. 3, below.

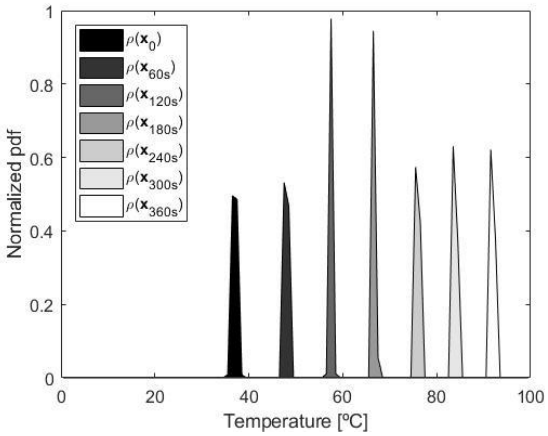

Figure 3. Evolution of the posterior probability density function in time

The evolution of the probability density function in Fig. 3 represents how likely is the value of the temperature at each time step, which is not deterministic. However, considering that the highest value of the probability density function at each time step represents the estimated temperature, deterministic values for this variable can be obtained.

In Fig. 4, a comparison of analytical solution, numerical solution and estimated temperatures is shown.

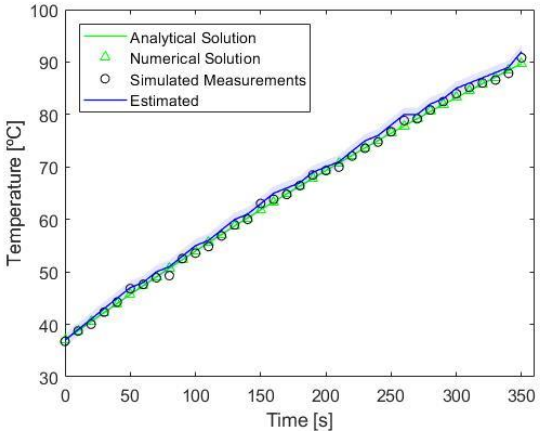

Figure 4. Analytical solution, numerical solution and estimated temperatures

As seen in Fig. 4, both analytical and numerical solutions are in good agreement. The measurements were generated with the numerical solution of the direct problem, with measurement errors modelled as additive and uncorrelated Gaussian variables, with zero mean and a constant standard deviation of 0.5°C, considered available with a frequency of 100Hz. The blue shaded region represents the confidence interval of 99%. The estimated temperatures also showed good agreement with both analytical and numerical solutions, suggesting that the application of the Optimal-Bayesian Filter, in this case, is a viable alternative in predicting the filtering states.

4.2 Kidney problem

A prior distribution for metabolic heat generation rate was specified by using a tool package for Matlab named COBRA, which allowed for the quantification of the energy source based on the renal consumptions of glucose and oxygen (Vlassis et al., 2014; Laurent et al., 2019).

The Monte Carlo simulation was used to generate a probability distribution of the total energy produced in the kidneys. For this simulation, it was necessary to use the COBRA tool package and the a priori distributions of renal oxygen and glucose consumption, shown in Tab. 1. The a priori distribution for renal glucose consumption was considered uniform, between the minimum and maximum values given by Stumvoll et al. (1995), while for renal oxygen consumption, prior distributions were taken as Gaussian distributions with the means presented by Brundin and Wahren (1994) and standard deviation of 1% of the means.

Table 1. Reference values used for the Monte Carlo analysis

	Mean	Minimum	Maximum	Standard Deviation
Oxygen (mole/min)	0.820	-	-	0.008
Glucose (mole/min)	1.84×10^{-4}	1.12×10^{-4}	2.88×10^{-4}	-

The histogram is not presented here for the sake of brevity, but each resembled a uniform distribution. Therefore, the priors for oxygen and glucose were assumed as uniform, with means and standard deviations obtained from the Monte Carlo simulation. The results obtained for the total energy were a uniform distribution, using 2.5×10^3 states in the Monte Carlo was $1.8221 \leq E_{Total} < 4.6847$ watts, with mean of 3.2571 and standard deviation of 0.8250.

To generate candidates for the state variable Q_m, it was also used the information that only 60% of the total energy produced in the kidneys is transformed into metabolic heat (Johnson and Knudsen, 1965), therefore

$$Q_m = 0.6E_{total}(1+w) \tag{30}$$

where E_{total} is the total energy of the kidney while w is a random number with Gaussian distribution, zero mean, and standard deviation of 10^{-2}. Again, the histogram is not presented here for the sake of brevity. The results obtained for the metabolic heat flux Q_m, using 2.5×10^3 states in the Monte Carlo was $1.0624 \leq Q_m < 2.8884$ watts. Quantitative information regarding $[\alpha, \beta, \gamma, \varphi, \psi]$ parameters can be found in Orlande et al. (2019).

To generate the simulated measurements, a decreasing ramp function was used, with variations between 2.8884 and 1.0624 W for $Q_m(t)$ where $t_f = 240s$, this case simulates a gradual drop in the heat generation rate, which in practice would represent a sharp reduction of the kidney's physiological functions. The measurement errors were modeled as additive and uncorrelated Gaussian variables, with zero mean and a constant standard deviation of 0.001 K (Brundin and Wahren, 1994). In order to avoid an inverse crime (Kaipio and Somersalo, 2004) the measurements were generated with a finite difference solution of the direct problem, while a Runge-Kutta solution was applied for the inverse problem. The measurements were assumed available with a frequency of 1000 Hz.

The results obtained for the kidney temperature and for the kidney metabolic heat generation via direct problem can be seen in Fig. 5. The squares in Fig. 5 represent the numerical solution for the temperature and for metabolic heat generation at times 0s, 60s, 120s, 180s and 240s, respectively.

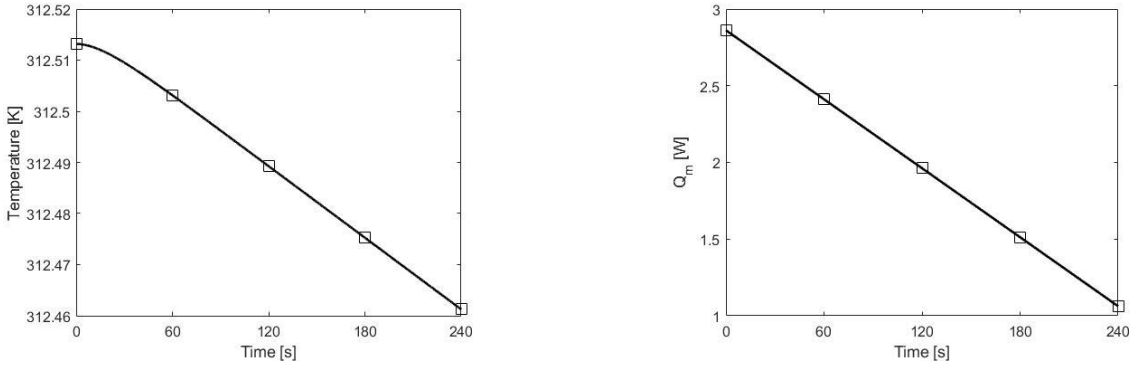

Figure 5. Direct problem results for kidney (a) temperature and (b) metabolic heat generation

For the estimations obtained with the Optimal-Bayes filtering, the initial probability density function $\rho(\mathbf{x}_0)$ was considered Gaussian $N((T_0, Q_{m,0}), \sigma_0^2)$ with $\sigma_0^2 = (0.0001; 0.01)$, the initial distribution is shown in Fig. 6.

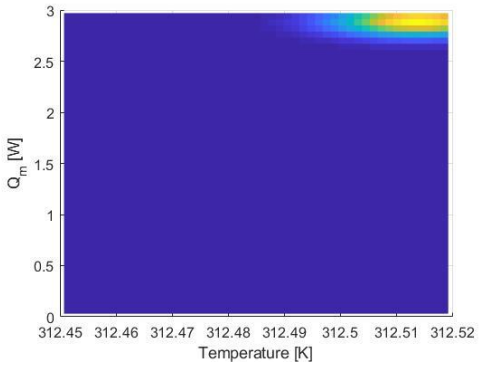

Figure 6. Initial probability density function for the kidney problem

The results obtained for the filtering states using two distinct standard deviation for the measurements, at specific times, represented for the squares in Fig. 5, can be seen in Fig. 7 and Fig. 8. The first standard deviation was provided by Brundin and Wahren (1994). The second standard deviation was considered to be 100 times bigger than the first one for comparison reasons, respectively.

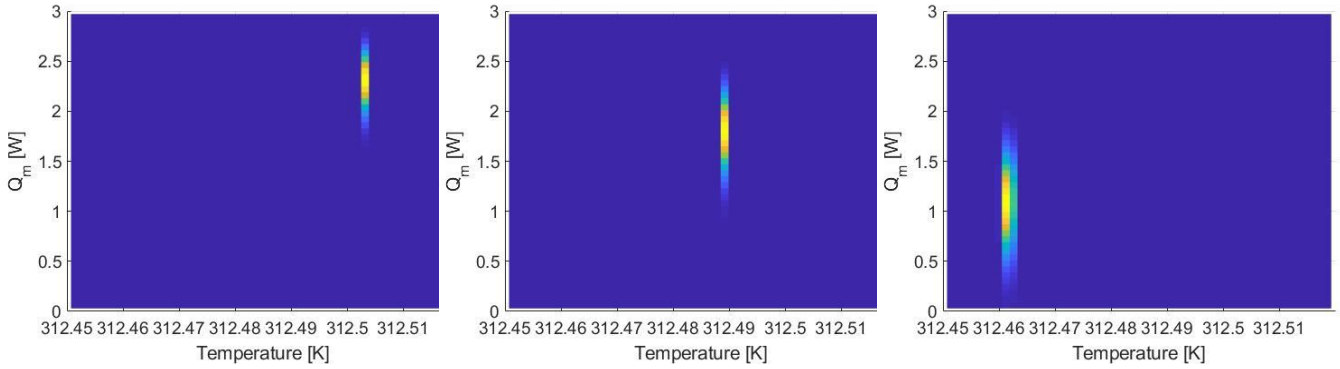

Figure 7. Filtering states at times (a) 60, (b) 120 and (d) 240s with measurement standard deviation of 0.001 K.

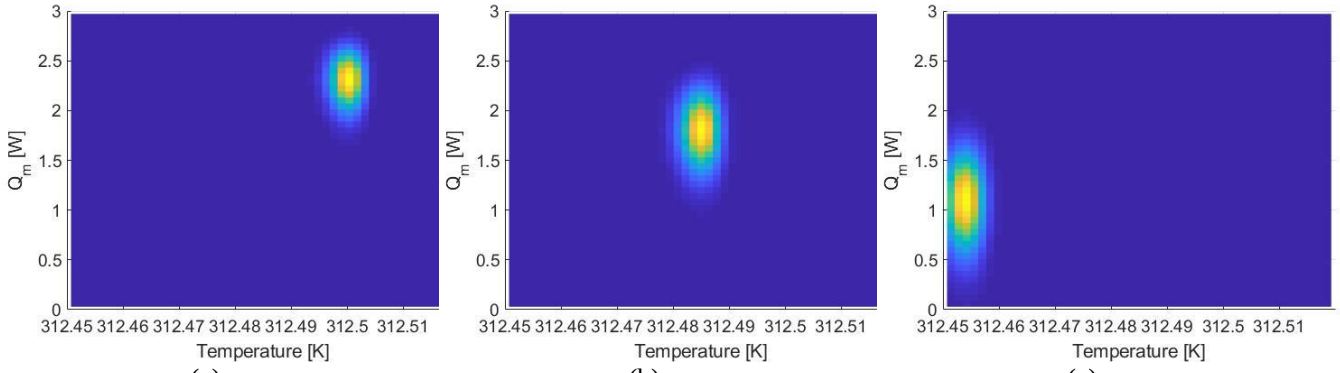

Figure 8. Filtering states at times (a) 60s, (b) 120s and (d) 240s with measurement standard deviation of 0.1K.

Figures 7 and 8 show that the estimated temperatures and renal metabolic heat generation coefficient are in good agreement with the numeric solution for the given time steps presented in Fig. 5a-b. However, the filtered states obtained considering a standard deviation for the measurements of 0.001 K, Fig. 7a-c, are closer to the numerical solution. Figure 8a-c shows that the area covered by the posterior probability density function is greater than the area covered in Fig. 7a-c, which is expected since the standard deviation of the measurements was changed from 10^{-3} to 10^{-1} K.

5. CONCLUSION

The Optimal sequential Bayesian filter implemented in this work requires solving the continuity equation for the states space, which was done using the upwind scheme of the finite volume method. The filter conserves probability, guarantees that the intermediate results are valid probability distributions and preserves positivity when the stability criteria is satisfied. It was shown that for low dimensional smooth systems its application is feasible. However, as the dimension of the states vector grows, the computational cost of the method grows exponentially.

In the laser heating problem, the estimated temperatures of the culture well were in good agreement with the numerical solution. This state variable is of great importance for the treatment of hyperthermia in tumor cells. In the kidney problem, the evolution of the posterior probability density on the plane $Q_m T$ over time was compared with the numerical solution and was found to produce probability densities in good accordance with the numeric values expected for the kidney temperature and metabolic heat generation function. Overall, the Optimal sequential Bayesian filter used in this work produced good estimations for both bioheat transfer problems proposed.

6. ACKNOWLEDGEMENTS

This work was supported by CNPq, CAPES – Finance Code 001, FAPERJ and FAPEAM.

7. REFERENCES

Arulampalam, M.S., Maskell, S., Gordon, N. and Clapp, T., 2002. "A Tutorial on Particle Filter for Online Non-linear/Non-Gaussian Bayesian Tracing". *IEEE Trans. Sig. Proc*., Vol. 50, pp. 174-188.

Brundin, T. and Wahren, J., 1994. "Renal oxygen consumption, thermogenesis, and amino acid utilization durin iv infusion of amino acids in man". *American Journal of Physiology-Endocrinology and Metabolism*, Vol. 267, No. 5, pp. E648-E655.

Fox, C., Dolgov, S., Morrison, M.E.K. and Molteno, T.C.A., 2019a. "Bayes-Optimal Filtering for Nonlinear Dynamical Systems". In *Inverse Problems, Design and Optimization Symposium*. Tianjin, China.

Fox, C., Norton, R.A., Morrison, M.E.K. and Molteno, T.C.A., 2019b. "Sequential Bayesian Inference for Dynamical Systems Using the Finite Volume Method". In: *2017 Matrix Annals*, pp. 13-23. Springer, Cham.

Fox, C., Morrison, M.E.K., Norton, R.A. and Molteno, T.C.A., 2018. "Optimal Non-linear Filtering Using the Finite Volume Method". *Phys. Rev. E Stat. Nonlin. Soft. Matter Phys*, Vol. 97, No. 1, 010201.

Guyton, A.C. and Hall, J.E., 2006. *Textbook of medical physiology*. PA:WB Saunders Company.

Jazwinski, A.H., 1970. *Stochastic Processes and Filtering Theory*. Academic Press, New York.

Johnson H. A., Knudsen K. D., 1965. "Renal efficiency and information theory". *Nature*, Vol. 206, pp. 930-931.

Kaipio, J. and Somersalo, E., 2004. *Statistical and Computational Inverse Problems*. Springer Science, New York, 1st edition.

Lamien, B., Orlande, H.R.B. and Eliçabe, G.E., 2017. "Particle Filter and Approximation Error Model for State Estimation in Hyperthermia". *Journal of Heat Transfer*, Vol. 139, pp. 012001.

Laurent, H. et al., 2019. "Creation and analysis of biochemical constraint-based models: the COBRA Toolbox, Nature Protocols", Vol. 3, No. 14, pp. 639-702.

Lutaif, N.A., Rocha, E.M., Veloso, L.A., Bento, L.M., and Gontijo, J.A.R., 2008. "Renal contribution to thermolability in rats: the role of renal nerves". *Nephrology Dialysis Transplantation*, Vol. 23, No. 12, pp. 3798-3805.

Orlande, H.R.B., Lutaif, N.A. and Gontijo, J.A.R., 2019. "Estimation of the kidney metabolic heat generation rate". *International Journal for Numerical Methods in Biomedical Engineering*, Vol. 35, No. 9, pp. e3224.

Orlande, H.R.B., 2015. *Tutorial 7: The Use of Techniques whitin the Bayesian Framework of Statistics for the Solution of Inverse Problems*.

Ozisik, M.N. and Orlande, H.R.B., 2000. *Inverse Heat Transfer: Fundamental and Applications*. Wiley & Sons, New York, 1st edition.

Patankar, S.V., 1980. *Numerical Heat Transfer and Fluid Flow*. Hemisphere Publishing Corporation, New York.

Ricquier, D., 2006. "Fundamental mechanisms of thermogenesis". *Comptes Rendus Biologies*, Vol. 329, pp. 578-586.

Stumvoll, M., Chingatalapudi. U., Perriello, G., Welle, S., Gutierrez, O. and Gerich, J., 1995. "Uptake and release of glucose by the human kidney. Postabsorptive rates and responses to epinephrine". *The Journal of Clinical Investigation*, Vol. 96, pp. 2528-2533.

Tang, Y. and McGoron, A.J., 2009. "Combined effects of laser-ICG photothermotherapy and doxorubicin chemotherapy on ovarian cancer cells". *Journal of Photochemistry and Photobiology B: Biology*, Vol. 97, No. 3, pp. 138-144.

Varon, L.A.B., Loiola, B.R., Abreu, L.A.S., Lamien, B., Silva, N.P., Orlande, H.R.B. and Santos, D.S, 2020. "Thermal Effect by Applying Laser Heating in Iron Oxide Nanoparticles Dissolved in Distilled Water". In *15th Mediterranean Conference on Medical and Biological Engineering and Computing*. Coimbra, Portugal. IFMBE Proceedings 76, pp.1-7.

Varon, L.A.B., Orlande, H.R.B. and Eliçabe, G.E., 2017. "Combined parameter and state estimation in the radio frequency hyperthermia treatment of cancer". *Numerical Heat Transfer*, Part. A, Vol. 70, No. 6, pp. 581-594.

Vlassis, N., Pacheco, M. and Sauter, T., 2014. "Fast reconstruction of compact context-specific metabolic network models". *PLOS Computational Biology*, Vol. 10, e1003424.

8. RESPONSIBILITY NOTICE

The authors are the only responsible for the printed material included in this paper.